

Configuration-Dependent Flow Structures and Localized, Anti-equilibration Motion in a
Quasi 1D Magnetic Fluid in Horizontal Field and Temperature Gradients

Jun Huang and Weili Luo¹

Department of Physics, University of Central Florida, Orlando, FL 32816

Tianshu Liu

Department of Mechanical and Aerospace Engineering, Western Michigan University

Kalamazoo MI 49008-5343

Abstract

In a quasi-one-dimensional magnetic fluid, both gravito-thermal and magneto-thermal convections were observed in a horizontal temperature gradient, applied field, and field gradient. The interplay between the two convective motions crucially depends on the relative orientation of the gradient of temperature to that of applied field. The magnetic field-induced flows either enhance the convective heat transfer when the gradients of temperature and field are parallel to each other, or suppress it when the two gradients are antiparallel, where the convection roll in zero field was replaced by two localized flows at the two ends of the sample cell. This localized flow structure inhibits the heat flow of approaching to thermal equilibrium in the system, causing the temperature difference across the sample to increase with applied fields. The drastically different effects of the field and the field gradient on the equilibration processes resulted from two totally different topological flow-structures for the two experimental configurations imply a profound bifurcation of solutions for the underlying physics.

¹ weili.luo@ucf.edu

One of the common heat transfer mechanisms is gravito-thermal convection where the hot fluid ascends due to buoyancy force and the cold fluid descends to replace the rising hot fluid. An applied magnetic field can drive a fluid to convective instability similar to gravity but it has the advantage of being more flexible in orientation as well as in magnitude comparing to gravity [1-6]. Finlayson [7] proposed in 1970 that if a vertical uniform magnetic field is applied on a ferromagnetic fluid along a temperature gradient, convective instability can result from the temperature-dependent magnetization, which gives rise to a temperature-dependent internal field whose gradient is a function of temperature gradient. A ferromagnetic fluid (ferrofluid) or magnetic fluid (MF) is a complex fluid with magnetic nanoparticles suspended in a non-magnetic solvent [2]. Because the magnetic susceptibility for a MF is usually several orders of magnitude larger than ordinary para- or dia- magnetic fluids, the magnetic field required for many intriguing phenomena is much smaller. Although magnetically induced convections in MF have been observed by several groups [8-13], the field is still in its early stage with very limited results. Due to its multi-components nature for a complex fluid, the interaction between the magnetic moments of particles in the fluid and the applied field could lead to rich new phenomena that are absent for single-component para- and dia- magnetic fluids [2, 14-15].

In this paper, we report our novel observations of peculiar flow patterns in a special quasi one-dimensional cell driven by magnetic body force originated from horizontal magnetic field, field gradient, and its interaction with the gravito-thermo convection induced by horizontal temperature gradient. We found that when the gradients of temperature and field are parallel to each other the zero-field gravito-thermal convection is transformed to a global vortex structure with increased circulation speed; while when these two gradients are antiparallel to each other the gravito-thermo convection is replaced with localized flows at the two ends of the sample with a saddle point in between. The “end” flows prevent the heat transfer from one side to another, causing the temperature difference across the sample increasing with increasing field, rendering the system further away from equilibrium. Understanding the underlying mechanism for this anti-equilibration phenomena not only shines light on far equilibrium phenomena such as atmospheric motions both on earth and on other planets and stars where there is a magnetic field such as origin of sunspots, lava

flows in magnetic fields, seismological phenomena such as earthquakes from convections inside the Earth, etc., but also provide ideas for field-controlled fluidic energy devices.

The sample is a quasi 1D MF consisting magnetic nanoparticles of 10 nm suspended in nonmagnetic solvent. The saturation magnetization of the sample is 55 Gs and the volume fraction of the particles is 1% [16]. The susceptibility of this diluted sample is 0.2 and the thermal conductivity is very close to that of the base carrier, kerosene [17]. For our dilute concentration, we can consider that the fluid exhibits super-paramagnetic behaviour. The sample cell in our experiment is made of Acrylic with the dimension 90mmx7.5mmx5.5mm with its long axis, the temperature gradient, applied magnetic field, and applied field gradient all in the horizontal direction that is perpendicular to the gravity. When horizontal heating and cooling are applied in zero field, the buoyancy force due to thermal expansion drives the system to convective instability.

In Fig. 1 we present our experimental set up. The two exactly matched sample cells are arranged side by side. Both are heated on the left side with electric heaters and cooled from right side with running coolant from a cold tank so that the temperature gradients in both cells are towards left. Two cells with separation of 12.2 cm were placed inside two electromagnetic poles. The spatial distribution of the field is symmetric about the centre with the field direction along the temperature gradient. The field gradients are toward the magnetic poles for the two cells so that for the left cell the gradients of temperature and the applied field are parallel (PL), for the right cell antiparallel (AP) to each other. In Fig. 2 we plot the temperature as function of time for different applied fields obtained from the thermocouples at the four corners of each sample cell, with Fig. 2(a) for parallel configuration (PLC) and Fig 2 (b) for antiparallel configuration (APC), respectively. The insets in both Fig. 2 (a) and Fig. 2 (b) show the labels for the thermocouple positions: LLT denotes one for left cell (PLC), left side (hot side), and the top position; LRB for left cell, right side (cold side), and bottom location; RRT for right cell (APC), right side (cold side), and top location, etc. Once the heating and cooling are applied at $t = 0$ sec, the convective flow starts [16]. The temperatures in the two samples reach steady states at $t \geq 1000$ sec. in zero field. Then the magnetic field was applied by steps: at $t = 2000$ s, 10mT was applied. We wait for 200 sec. in this field; then 20mT was applied for 200sec., then 30mT, etc. At each step the field was increased by 10 mT. The field values here refer to the ones measured at the magnet

poles; therefore, they are the maximum values for that applied field along the axis of the two poles. For PLC, applying field reduces the temperature difference across the sample cell (from LLT to LRT; LLB to LRB) as well as from top to bottom of the cell (LLT to LLB and LRT to LRB) as shown in Fig. 2 (a); for APC, the applied field enhances the temperature difference across the sample (RLT to RRT; RLB to RRB), clearly indicating that the applied field could drastically altered the convective heat transfer, depending on the configuration of the experiment.

To understand the underlying mechanism, we need to know flow pattern as function of field. For the *opaque* MF, we have adopted an indirect imaging process that involves two different techniques: 1) the trace-particle velocimetry (TPV). Since the concentration of the particles is only 1% in volume fraction, it is a good approximation to assume that the flow pattern in *zero field* for MF is essentially same as that of base fluid. We can image the flow velocity in *transparent* base fluid by TPV in zero field. Cenosphere grade 500 particles were added to base fluid as trace particles [18]. The streamlines obtained by analysing the time-dependent flow velocity in zero field was plotted in Fig 3 as the base flow. A single convective roll as well as Kevin-Helmholtz instabilities [1] at the interface between the two opposite flows along the horizontal direction are clearly visible. 2) The second method is the temperature sensitive paint (TSP) technique [19] for MF, in which a thin layer of florescent polymers was painted on the outer surface of cell. Using ultraviolet light to shine on the surface of the cell, the intensity of florescent light is proportional to the local temperature. After the intensity information of TSP was collected by camera, we can get the temperature distribution from a calibration standard. Then the optical flow technique was used to analyse the time dependence of the temperature distribution that is related to the flow velocity of the fluid [20]. Applying the optical flow method to a temperature change induced by a field applied as a perturbation, one can obtain the flow velocity variation field for the sample in different magnetic fields. Then the flow velocity variation as the perturbation was added to the base flow to reconstruct the complete velocity field for that magnetic field at certain time.

In Fig 3(a) and(b), the streamlines are plotted for PLC and APC, respectively, in applied field of $B_{\max} = 20\text{mT}$, 40mT , 60mT , and 80mT . We used the field value measured at poles, B_{\max} , to indicate every field applied. Even for low field strength, the flow pattern has

changed considerably comparing to that of zero field. For PLC, convective boundary layer flow in zero field has been replaced by a large vortex whose centre shifts to the higher field and higher temperature side with increasing field. For APC, the applied field “separates” the circular flow in zero field into two “localized” flows at two ends of the sample cell. The “saddle” point between the two end flows shifts to the higher field, low temperature side with increasing field. For both configurations, we observed “opening” at the ends of the cell, suggesting the crossover from two- to three-dimensional flow in applied fields. When there is a temperature gradient in the system, both gravity and magnetic force can drive a fluid to convective instability: the gravito-thermal and magneto-thermal convective motions. The Rayleigh number for gravito-thermal convection is defined by [1-2, 21-22]:

$$Ra = \frac{c_p \rho^2 g \beta \nabla T l^4}{\eta k} \quad (1)$$

where c_p is specific heat (1.84×10^3 J/kg K), ρ the density of the fluid (0.87×10^3 kg/m³), g is gravitational acceleration (9.8 m/s²), β the thermal expansion coefficient (0.85×10^{-3} K⁻¹), l is the length scale of importance in the study, ∇T is the temperature gradient across the length scale l ; and η is dynamic viscosity (8.5×10^{-3} kg/m s), and k is thermal conductivity (0.15 W/m K) [14]. We assume these parameters are roughly constants. The convective flow driven by magnetic body force is characterized by the magnetic Rayleigh number [2, 7]:

$$Ra_m = \frac{c_p \rho \mu_0 K \nabla T \nabla H l^4}{\eta k} \quad (2)$$

where μ_0 is vacuum permeability ($4\pi \times 10^{-7}$ N/A²), ∇H the field gradient, K Pyromagnetic coefficient: $K = \left(\frac{\partial M}{\partial T} \right)_H$. To calculate K values in different fields, we solved the equation for magnetization self-consistently: $M = M_s L(\alpha)$, where M_s is the saturation magnetization and $L(\alpha)$ the Langevin function; $\alpha = \frac{m \mu_0 (H+M)}{kT}$, m is the magnetic moment for one particle and H is the local field. The inter-particle interaction is not important for our low concentration. For the quasi 1D geometry of our sample, $H(x) \cong H_o(x)$ with $H_o(x)$ the applied field. After obtaining magnetization as a function of temperature and field, Pyromagnetic coefficient, K , was calculated. Since the fluid motion in zero field is boundary layer flow and the field has the more pronounced effect on the two boundary walls perpendicular the field, the meaningful length scale on which the temperature gradient is taken should be proportional to the layer thickness of the boundary layer. Thus, l should be the height of the cell [22].

Within this small length scale both gradients of temperature and field can be expressed as: $\nabla T = \frac{\Delta T}{l}$, $\nabla H = \frac{\Delta H}{l}$. Where ΔT and ΔH can be obtained by experiment.

In Fig. 4 we plot both gravito-thermal and magneto-thermal Rayleigh numbers as a function of applied field, B [23], taking into account the field dependence of the local temperature and the Pyromagnetic coefficient, while keeping other parameters in (1) and (2) as constants [24-25]. Because temperature gradients at the hot and cold sides are different, we plot them separately for both configurations. Fig 4 (a) and (b) are the Rayleigh numbers for the hot and cold sides of PLC and (c) and (d) are similar plots for APC. At the hot side of PLC (Fig 4 (a)) and cold side of APC (Fig. 4(d)), the magnetic Rayleigh numbers, Ra_m , are always larger than the thermal Rayleigh numbers, Ra , due to the proximity to the magnetic poles where the field strengths and the field gradients are the highest. At the cold side of PLC (Fig.4 (b)) and hot side of APC (Fig. 4 (c)), the magnetic Rayleigh numbers, Ra_m , are smaller than the thermal Rayleigh numbers, Ra , for lower fields. Then the two Rayleigh numbers cross at the magnetic field $B_{\max} \approx 30$ mT, beyond which the magneto-thermal convection dominates. These features indicate that at the lower fields we can observe the co-existence of gravito-thermal and magneto-thermal convections and we are able to separate them by tuning the strength of the applied field to higher values.

In Fig 5 (a) we plot vertical velocity component averaged across the vertical coordinate, U_y , versus a specific location along the horizontal direction, x , for PLC and APC in zero and applied fields. The increment of field is 20 mT. Fig 5(b) are the similar plots but for horizontal velocity component averaged across the vertical coordinate, U_x , versus x . For both configurations, the increases in magnitudes of U_y and U_x are larger at the ends of the sample cell, especially at the sides where the field and field gradient are smallest, possibly due to the decrease of the susceptibility at the higher fields. For APC, because of the heat energy in the system is not communicated between the hot and cold sides, the field-induced localized thermal energy was transferred to kinetic energy, whose values are even larger than the PLC at the ends.

In summary, two drastically different types of temperature changes as a function of field were observed in our quasi one-dimensional fluid sample, depending on the relative orientations of temperature gradient vs. field gradient. The discrepancy originates from the

dissimilar flow structures induced in field. These very different configuration-dependent flows point to a novel, important bifurcation of solutions for the fluid dynamic equations as a function of relative orientation of the two gradients, for which there is no existing theory. The solutions manifest in PLC as a faster speed along the same circulation direction as in zero field, enhancing the heat transfer in the system; while for ALC, the magnetic driving force led to localized flows at the ends of the sample that “trapped” the heat (or cold) energy, strongly inhibiting convective heat transfer from hot to cold side. This localization effect prevents the approaching equilibrium in the fluid, rendering the temperature across the sample to increase with field. This implies that the process for “heat flows from the hot to the cold side” can be halted by the magnetic driving force, $\mathbf{f} = \nabla \left(\frac{1}{2} H^2 \rho \frac{\partial \chi}{\partial \rho} \right) - \frac{1}{2} H^2 \nabla \chi$ [23, 26], where H and χ are the local field and susceptibility, both depending on the local temperature; ρ is the density of the fluid. The phenomena reported here, including the flow patterns for two configurations, as far as we know, have not been observed or studied before. For our experimental situation where temperature T , magnetic field B , and concentration of particles ρ are all function of space as well as time, it is a challenge for theorists to find general solutions for the problem. At the current stage, experimental studies are the important pathways to provide crucial information and insight for the underlying physics that has diverse implications in non-equilibrium phenomena. On the application side, the field controlled heat transfer can be used for improving heat-removing efficiency in devices such as transformers [27], micro-electronics [28], and new generation of field-controlled energy-saving devices.

In our experimental time scale the effect due to magneto-diffusive convection is not important due to the long time needed to establish the mass gradients [29-32].

Acknowledgement

We thank Dr. Kuldeep Raj from Ferrotech for providing the sample MF 905 used in this experiment.

References

- [1] See, for example, S. Chandrasekhar, *Hydrodynamics and Hydromagnetic Stability*, (Oxford University Press, New York, 1966).
- [2] R. Rosensweig, *Ferrohydrodynamics*, (Dover Publications, Inc. 1997).
- [3] D. Braithwaite, E. Beaunon, and R. Tournier, "Magnetically controlled convection in a paramagnetic fluid," *Nature (London)* **354**, 134 (1991).
- [4] J. R. Carruthers and R. Wolf, "Magneto-thermal Convection in Insulating Paramagnetic Fluids," *J. Appl. Phys.* **39**, 5718 (1968).
- [5] H. Nakamura, T. Takayama, H. Uetake, N. Hirota, K. Kitazawa, "Magnetically Controlled Convection in a Diamagnetic Fluid," *Phys. Rev. Lett.* **94**, 144501(2005).
- [6] T. Bednarz et al., "Experimental and numerical analyses of magnetic convection of paramagnetic fluid in a cube heated and cooled from opposing verticals walls." *Int. J. Thermal Sciences*, **44**, 933 (2005).
- [7] B. A. Finlayson, "Convective instability of ferromagnetic fluids." *J. Fluid Mech.* **40**, 753 (1970).
- [8] L. Schwab, U. Hildebrandt, and K. Stierstadt, "Magnetic Bernard Convection," *J. Magn. Magn. Mater.* **39**, 113 (1983).
- [9] L. Schwab and K. Stierstadt, "Field-Induced Wavevector-Selection in Magnetic Bernard Convection" *J. Mag. Mag. Mat.* **65**, 315 (1987).
- [10] A.A. Bozhko, G.F. Putin, "Instabilities and spatial-temporal patterns in magnetic fluid convection. In: Proceedings of the 4-th International Pamir Conference on Magneto-hydrodynamic at Dawn of Third Millenium (Presqu'ile de Giens, France, 2000), **1**, 81–86.
- [11] A. A Bozhko and G. F. Putin, "Heat transfer and flow patterns in ferrofluid convection." *Magnetohydrodynamics* **39**, 147 (2003); A. A. Bozhko, P. V. Bulychev, G. F. Putin, and T. Tynjala, "Spatio-Temporal Chaos in colloid Convection." *Fluid Dynamics*, **42**, No.1, pp24-32, 2007.
- [12] E. Blums, Yu A. Mikhailov, and R. Ozols, *Heat and Mass Transfer in MHD Flows*, (Singapore, World Scientific, 1987).
- [13] S. Suslov, A. A. Bozhko, G. F. Putin, and A. S. Sidorov, "Interaction of gravitational and magnetic mechanisms of convection in a vertical layer of a magnetic fluid." *Physics Procedia* **9**, 167 (2010).
- [14] E. Blums, A. Cebers, and M.M. Maiorov, *Magnetic Fluids*. (Waterde Gruyter, 1997).
- [15] S. Odenbach and S. Thurm, *Magnetoviscous Effects in Ferrofluids*. ed. by S. Odenbach LNP 594, pp185-201 (Springer, 2002). M.I. Shliomis, *JETP* **34**, 1291 (1972).
- [16] Jun Huang and Weili Luo "Heat Transfer Through Convection in a Quasi-One-Dimensional Magnetic Fluid." *Journal of Thermal Analysis & Calorimetry*, **113**, 449 (2013).
- [17] V. E. Fertman, *Magnetic Fluid Guide Book--Properties and Applications*. (Hemisphere Publishing Corporation, 1990).
- [18] The cenosphere grade 500 particles used in TPV is 1% in volume and 180 micrometers in size.
- [19] Tianshu Liu and J.P. Sullivan, *Pressure and Temperature Sensitive Paints*, (Springer Verlag, 2005).
- [20] Tianshu Liu and Lixin Shen, "Fluid Flow and Optical Flow." *J. Fluid. Mech.* **614**, 253, (2008).
- [21] Adrian Bejan, *Heat Transfer* (John Wiley & Sons, Inc., 1993).
- [22] L. D. Landau and E. M. Lifshitz, *Fluid Mechanics*, (Pergamon Press, 1987).

- [23] Local applied field $B(x) = \mu_0 H(x)$.
- [24] Sergey A. Suslov, "Thermomagnetic convection in a vertical layer of ferromagnetic fluid", *Physics of Fluids*, **20**, 084101 (2008).
- [25] A.V. Belyaev and B. L. Smorodin, "The stability of ferrofluid flow in a vertical layer subject to lateral heating and horizontal magnetic field." *J. Magn. Magn. Mater.* **322**, 2596-2606 (2010).
- [26] F. Bakuzis, Kezheng Chen, Weili Luo, Hongzhang Zhuang, "Magnetic Body Force." *International Journal of Modern Physics B*, **19**, 1205-1208 (2005).
- [27] Raj K., Moskowitz R., Ferrofluid-cooled electromagnetic device and improved cooling method, US Patent number: 5462685, 1995
- [28] E. Blums, A. Mezulis, and G. Kronkalns, "Magnetoeconvective heat transfer from a cylinder under the influence of a nonuniform magnetic field." *J. Phys. Condens. Matter* **20**, 204128 (2008).
- [29] S. Odenbach, "Convection driven by forced diffusion in magnetic fluids." *Phys. Fluids* **6**, 2535 (1994).
- [30] E. Blums, A. Mezulis, and G. Kronkalns, "Magnetoeconvective heat transfer from a cylinder under the influence of a nonuniform magnetic field." *J. Phys. Condens. Matter* **20**, 204128 (2008).
- [31] N.V. Tabiryan and Weili Luo, "Soret feedback in thermal diffusion of suspensions." *Phys. Review E*. **57**, 4431 (1998).
- [32] Tengda Du and Weili Luo, "Nonlinear Optical Effects in Ferrofluids induced by Temperature and Concentration Crosscoupling." *Appl. Phys. Lett.* **72**, 272 (1998).

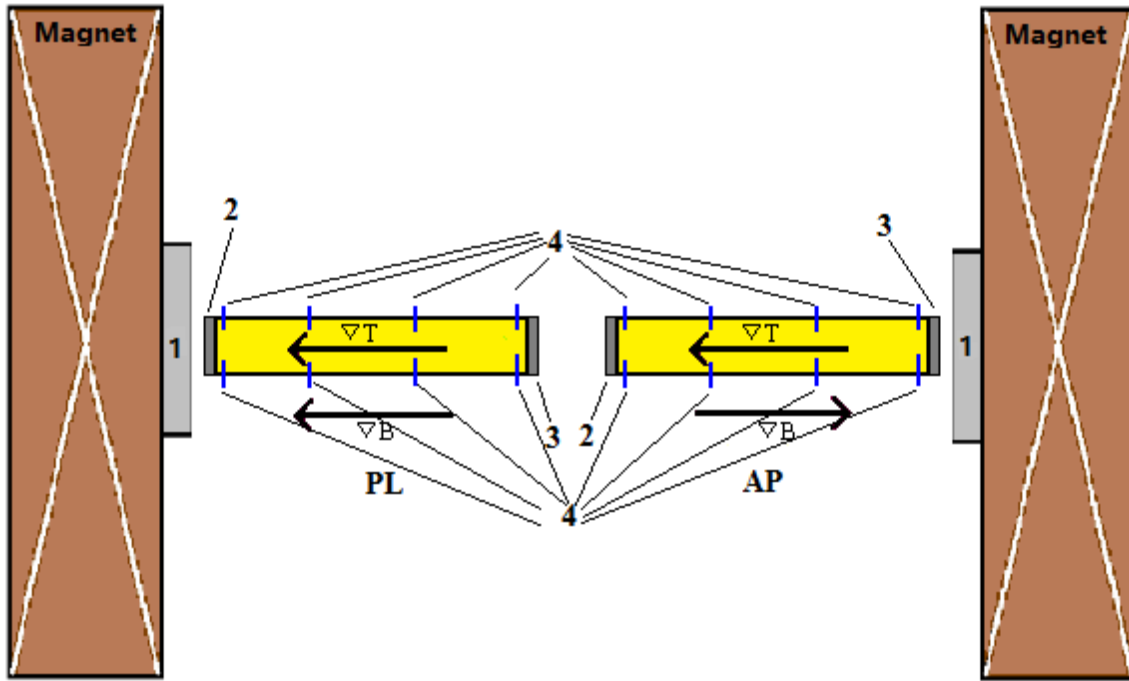
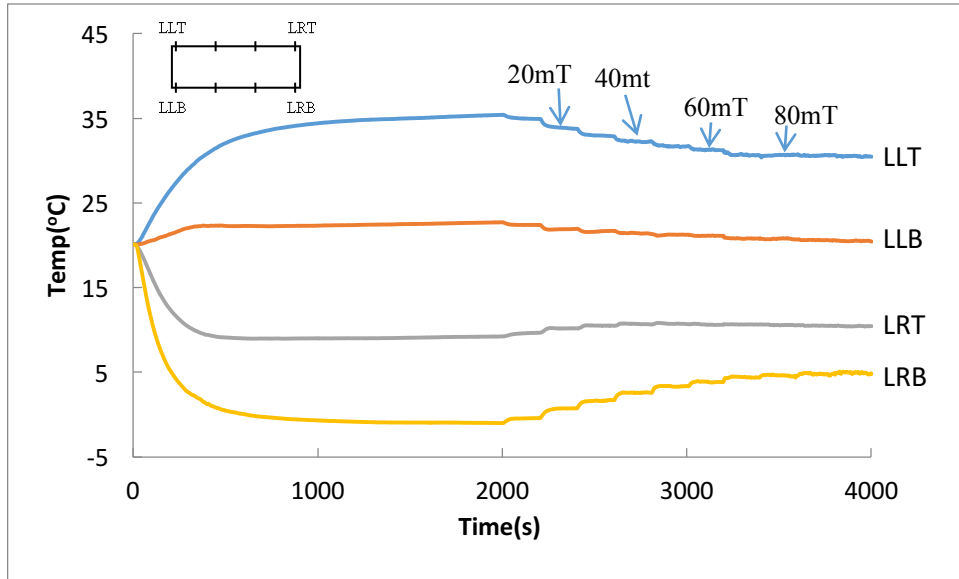
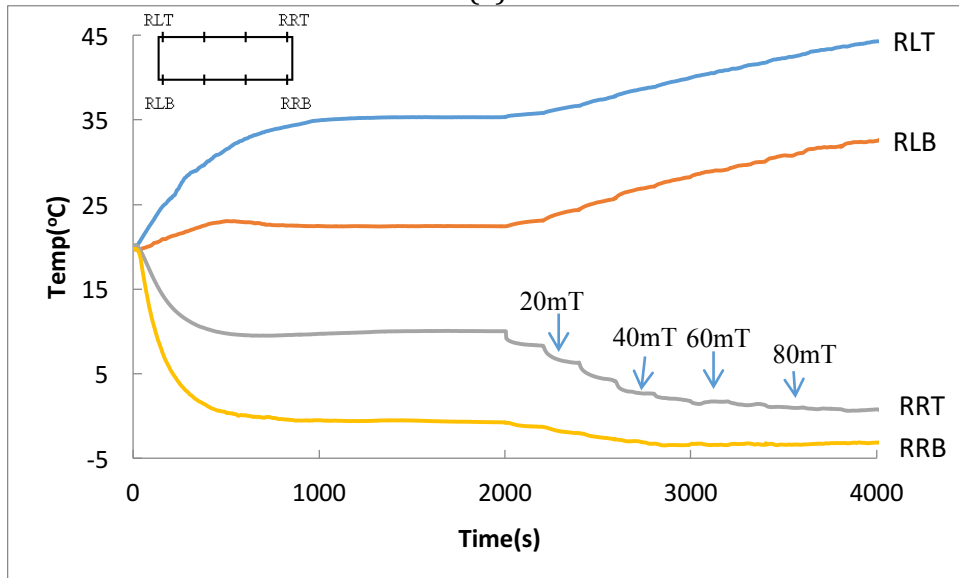


Fig. 1. Experimental Set up. 1: magnet poles; 2: electric heaters for both cells; 3: the cooling fluid running through the right sides of the both cells; 4: 8 thermocouples for each sample cell to monitor the temperature at top and bottom of the cell. For the left cell, the gradients of temperature and field are parallel to each other (PL), and for the right cell, antiparallel to each other (AP).

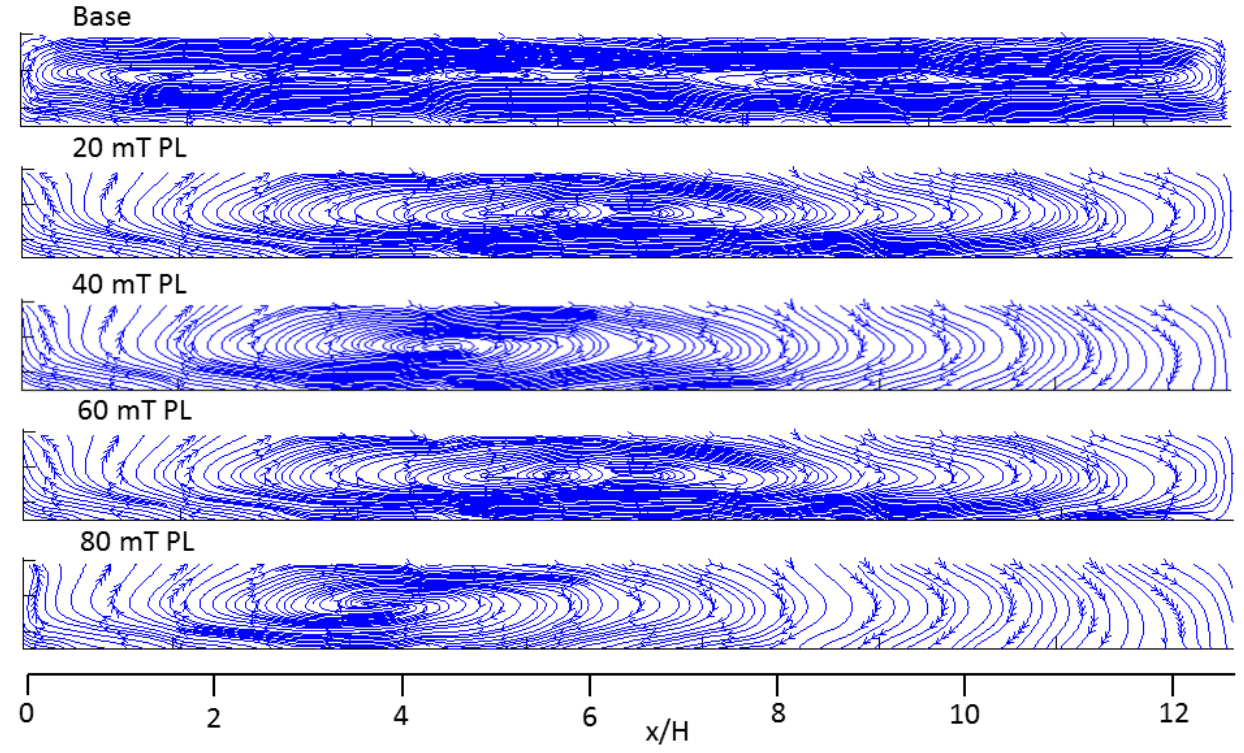


(a)

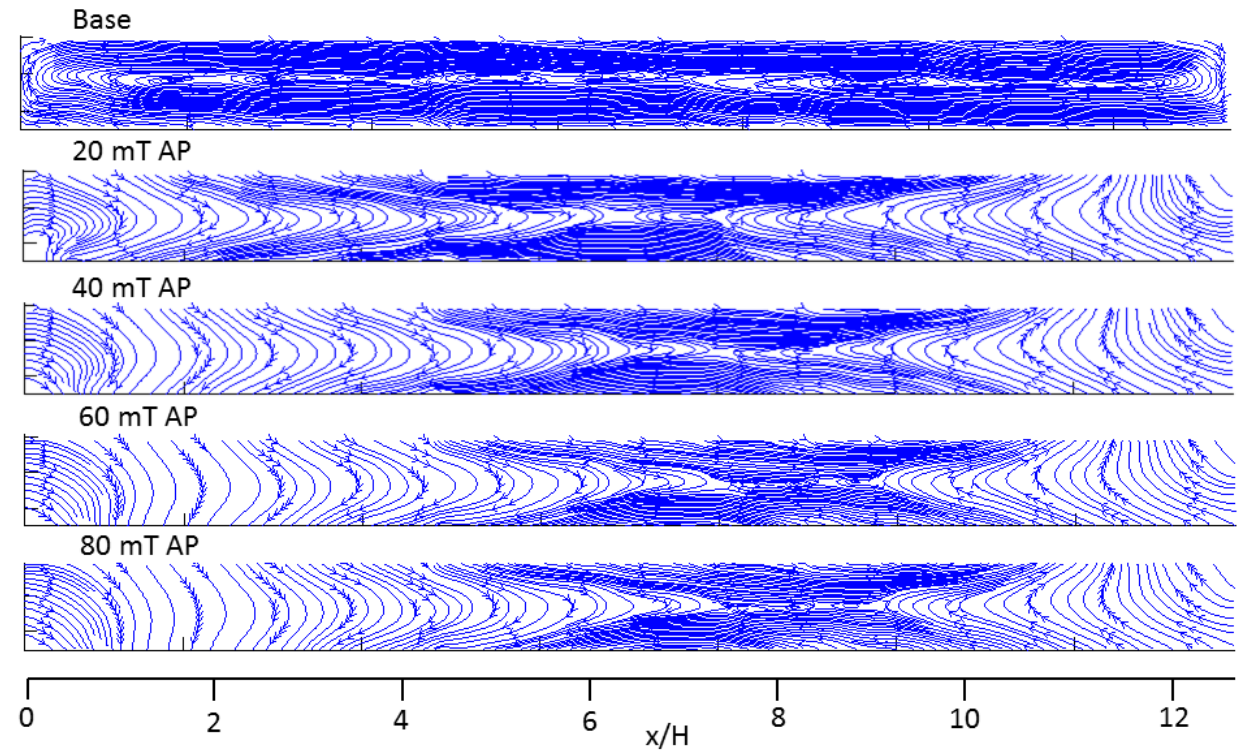


(b)

Fig 2. Temperature measured by thermal couples at the four corners of each sample cell as a function of time for (a) parallel (PLC) and (b) antiparallel (APC) configurations in zero field from 0-2000 sec. and their changes when fields were applied afterward. The insets show the labels for positions of the four thermal couples in each cell.



(a)



(b)

Fig 3. Streamline patterns for (a) PLC and (b) APC in fields of $B_{\max} = 20\text{mT}$, 40mT , 60mT , and 80mT . The horizontal axis is scaled by the vertical height of the sample cell, H .

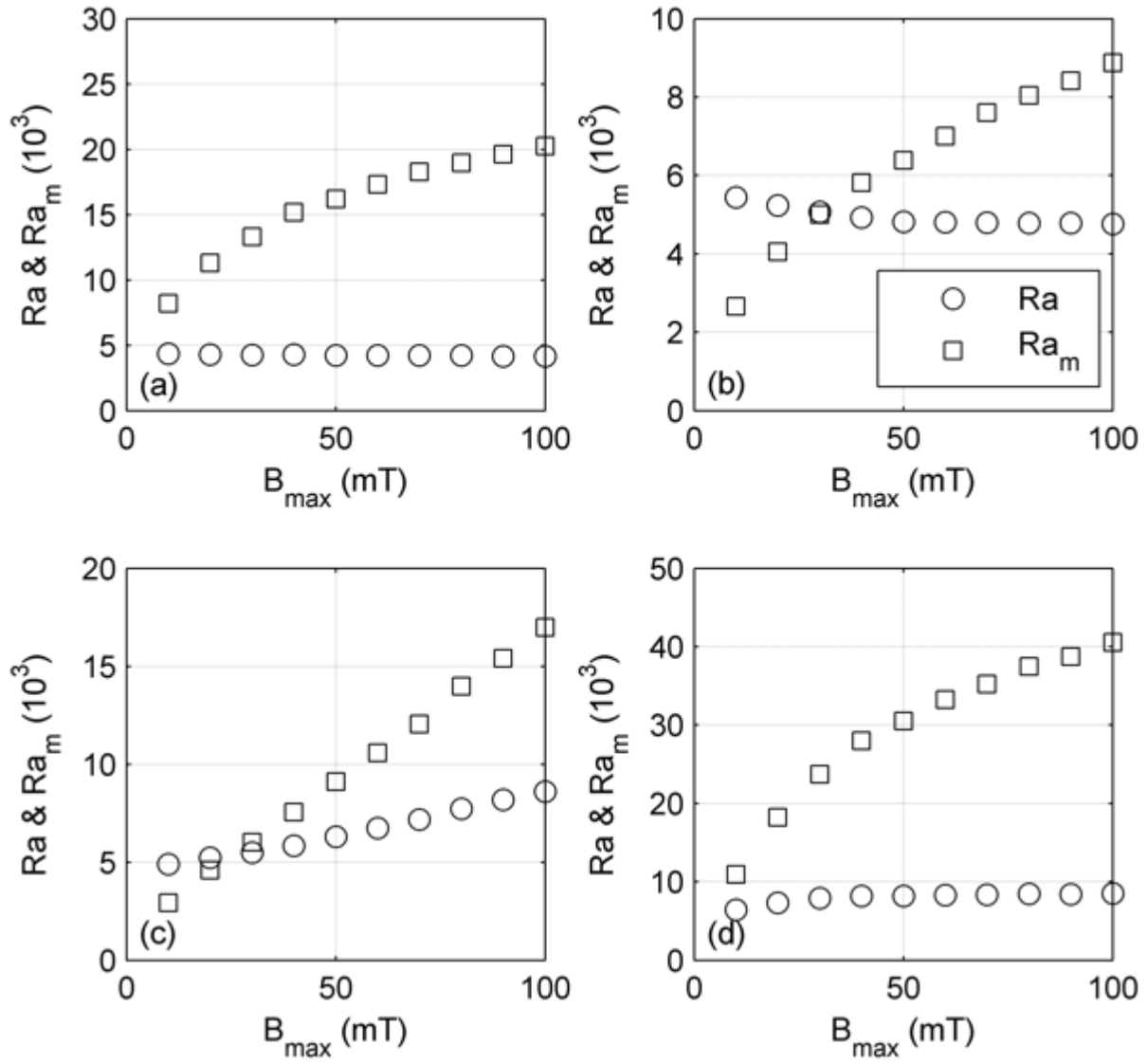


Fig. 4. Rayleigh number Ra (circle) and magnetic Rayleigh number Ra_m (square) as a function of the applied magnetic field for PLC at (a) hot side and (b) cold side, and for APC at (c) hot side and (d) cold side.

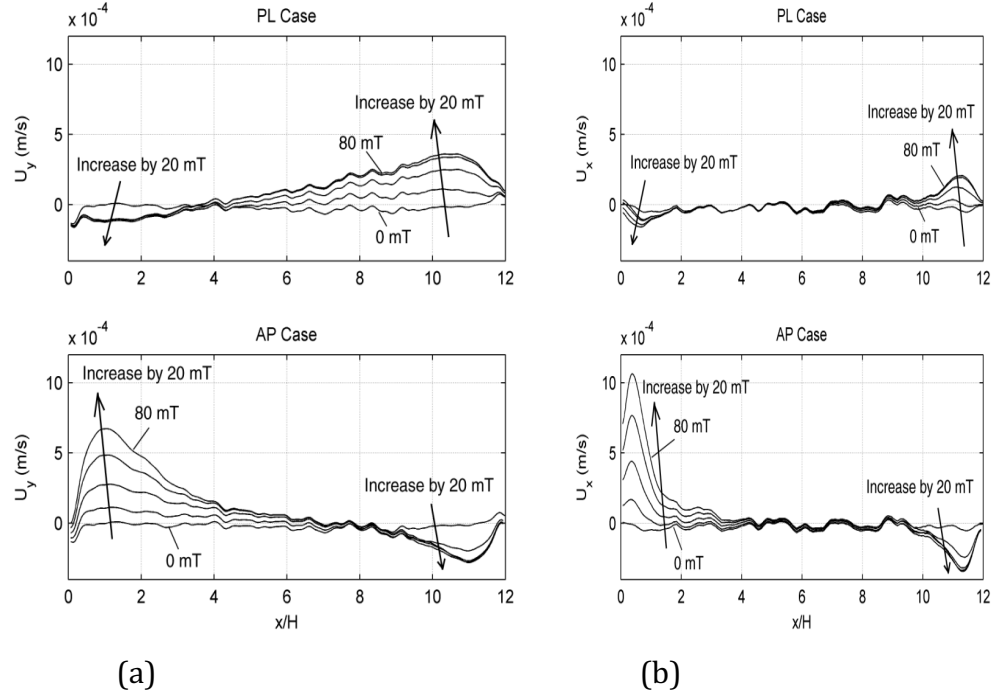


Fig. 5. The profiles of (a) vertical and (b) horizontal velocity components averaged across the vertical coordinate for parallel and antiparallel configurations. The horizontal axis is scaled by the vertical height of the sample cell, H .